Received: 26 October 2020 | Accepted: 21 December 2020

DOI: 10.1002/prp2.715

ORIGINAL ARTICLE

Biological features, gene expression profile, and mechanisms of drug resistance of two- and three-dimensional hepatocellular carcinoma cell cultures

Nan Mei | Ni Zhao | Tao Tian | Min Jiao | Chunli Li

Department of Medical Oncology, The First Affiliated Hospital of Xi'an Jiaotong University, Xi'an, Shaanxi Province, People's Republic of China

Correspondence
Chun-Li Li, Department of Medical Oncology, The First Affiliated Hospital of Xi'an Jiaotong University, Xi'an 710061, Shaanxi Province, People's Republic of China.
Email: chunli5158@163.com

Funding information
This work was supported by the Natural Science Foundation of Shaanxi Province (No. 2017JM8033), the Fundamental Research Funds for the Central Universities (No. xjj2017048), and the Scientific Research Fund Project of The First Affiliated Hospital of Xi'an Jiaotong University (No. 2016QN-02).

Abstract

Hepatocellular carcinoma (HCC) is a common malignant tumor with insidious onset and rapid progression. Its treatment is often difficult owing to tumor resistance. In this study, we aimed to understand the different biological characteristics, gene expression profiles, and drug resistance mechanisms of HCC cells cultured under different conditions. A conventional adherence method and a liquid overlay technique were used to prepare two- and three-dimensional cultures of Bel-7402 and 5-fluorouracil (5-Fu)-resistant Bel-7402 (Bel-7402/5-Fu) cells. Morphological characteristics were assessed via microscopy, and cell cycle distribution and apoptotic rate were obtained using flow cytometry. Cell sensitivity to different concentrations of drugs was detected with 3-(4,5-dimethylthiazol-2-yl)-2,5-diphenyltetrazolium bromide assays. Gene expression profiles and signal transduction pathways of Bel-7402 and Bel-7402/5-Fu cells under different culture conditions were determined using gene chips. Cells in three-dimensional culture were suspended and they grew into dense multicellular spheroid (MCS) structures, aggregating with each other. In contrast to cells in the two-dimensional culture, cell cycle arrest was observed in MCSs. The sensitivity of Bel-7402 cells in the two-dimensional culture to drugs at high concentrations was significantly higher than that of cells in the three-dimensional culture ($p < .05$). The apoptotic rate of Bel-7402 and Bel-7402/5-Fu cells was also higher in the two-dimensional culture ($p < .05$). Signal transduction pathway analysis showed that after Bel-7402 cells acquired resistance to 5-Fu, CCND1, MCM2, and MCM3 gene expression was upregulated in the G1 to S cell cycle control signal transduction pathway, CDKN1C and CCNG2 gene expression was downregulated, and MCM2 and MCM3 gene expression was upregulated in the DNA

Abbreviations: 5-Fu, 5-fluorouracil; ANXA3, annexinA3; Bel-7402/5-Fu, 5-Fu-resistant Bel-7402; CCND1, cyclin D1; CCNG2, cyclin G2; CDDP, cisplatin; CDKNIC, cyclin-dependent kinase inhibitor 1C; cRNA, chromosomal RNA; CSC, cancer stem-like cell; CTLA-4, cytotoxic T-lymphocyte-associated protein 4; DFS, disease-free survival; DLD-1, human colon adenocarcinoma cells; eEF1A1, eukaryotic translation elongation factor 1A1; EGFR, epidermal growth factor receptor; FOXO3, forkhead box O3; GAPDH, glyceraldehyde-3-phosphate dehydrogenase; GEO, gene expression omnibus; HCC, hepatocellular carcinoma; HNSCC, head and neck squamous cell carcinoma; HOXB2, homeobox B2; JAB1, Jun activation domain binding protein 1; LCSC, liver cancer stem cell; MCM2, minichromosome maintenance protein 2; MCM3, minichromosome maintenance protein 3; MCR, multicellular resistance; MCS, multicellular spheroid; MDR, multidrug resistance; MIG-6, mitogen-inducible gene 6; MMC, mitomycin; MTT, 3-(4,5-dimethylthiazol-2-yl)-2,5-diphenyltetrazolium bromide; NOTCH1, Notch 1 Signaling pathway; NOTCH3, Notch 3 Signaling pathway; OS, overall survival; PCNA, proliferating cell nuclear antigen; PCR, polymerase chain reaction; PD-1, programmed cell death-1; PD-L1, programmed cell death Ligand 1; p-ERK, phosphorylated ERK; PI, propidium iodide; PTX, paclitaxel; RNA, ribonucleic acid; SEM, scanning electron microscopy; STAT1, signal transducer and activator of transcription 1; TCGA, the cancer genome atlas; TEM, transmission electron microscopy; TFFI, trifoliate factor family.

replication signal transduction pathway. Therefore, the liquid overlay technique is a simple, low-cost procedure to successfully construct three-dimensional culture models of HCC. This study provides new information and methods for exploring the molecular mechanisms of liver cancer resistance, clinical treatment, development of molecular information, and interventional prevention.

KEYWORDS
gene expression profile, hepatocellular carcinoma, multicellular resistance, multicellular spheroids, signal transduction pathway, three-dimensional culture

1 | INTRODUCTION

Primary hepatocellular carcinoma (HCC) is one of the most common malignant tumors, ranking 6th in incidence and 2nd in mortality worldwide.[1] Chemotherapy is an effective treatment for advanced liver cancer patients, and 5-fluorouracil (5-Fu) is often used as the first-line chemotherapy drug for these patients. However, during the course of treatment, the development of multidrug resistance by HCC cells leads to their poor sensitivity to chemotherapy, one of the important reasons for the failure of HCC treatment. Therefore, the problem of drug resistance profoundly affects the efficacy of chemotherapy and the prognosis of patients. At present, the mechanism of 5-Fu resistance in liver cancer is not fully understood.

In research on cancer treatment resistance, most of the experiments are based on two-dimensional cultures of both stable cell lines and patient-derived primary tumor cells.[2] Nevertheless, in vivo, solid tumors are three-dimensional cell populations, and this three-dimensional structure leads to the development of a resistance mechanism in tumor cells called multicellular resistance (MCR), which may be the main reason for treatment resistance of cells in vivo.[3]

Therefore, in this study, we used gene chip and other techniques to analyze the cell biological characteristics, gene expression profiles, and signal transduction in Bel-7402 and 5-Fu-resistant Bel-7402 (Bel-7402/5-Fu) cell lines cultured under different conditions (two- and three-dimensional cultures), so as to further explore the drug resistance mechanism of liver cancer cells.

2 | MATERIALS AND METHODS

2.1 | Cell culture

Cells were maintained either in two-dimensional cultures according to the conventional adherence method or in three-dimensional cultures using a liquid overlay technique (agarose anti-adherent method). The human hepatocyte cancer cell lines Bel-7402 and Bel-7402/5-Fu were purchased from Nanjing Kaiji Biotechnology Development Co., Ltd. Bel-7402 and Bel-7402/5-Fu cells were cultured in RPMI 1640 (GIBCO) supplemented with 10% fetal bovine serum, 10% fetal calf serum, 100 U/ml penicillin, and 100 U/ml streptomycin. All cells were routinely cultured at 37°C in a 5% CO_2 (FORMA) environment. Approximately 0.8 ml of melted 2% agarose solution (Biowest, Hispanic) was uniformly coated on the bottom of a 50-ml culture bottle, approximately 2–3 mm thick, and allowed to cool into a gel. Cell suspensions at a density of (2–4) × 10^5/ml were added to a culture flask with agarose at its base and cultured at 37°C, 5% CO_2 (FORMA), and saturated humidity. Bel-7402/5-Fu cells were continuously cultured in medium containing 5-Fu at 2000 ng/ml.

TABLE 1 Drug concentration was determined with MTT sensitivity in Bel-7402 cells

Experimental drug	Drug concentration (mg/L)[a]				
5-Fu	6.25	12.5	25	50	100
CDDP	1.25	2.5	5	10	20
MMC	0.25	0.5	1	2	4
PTX	1	2	4	8	16

[a]The above drug concentration refers to the blood peak concentration and was set after preliminary experiments.

2.2 | Cell morphology

Cell morphology was evaluated using light microscopy (Leica) and scanning electron microscopy (SEM) (Beijing Science Instrument Center, Co. LTD). The structure of MCS and intercellular connections was evaluated using transmission electron microscopy (TEM) (HITACHI).

2.3 | Drug sensitivity test

Sensitivity of two-dimensional and three-dimensional cultured Bel-7402 and Bel-7402/5-Fu cells to 5-Fu, CDDP, MMC, and PTX was determined using MTT assays (Sigma). Bel-7402 and Bel-7402/5-Fu cells were inoculated into 96-well plates and precoated with 2% agarose at 150 μl/well, and cultured for 24 h for logarithmic growth and MCS formation. A volume of 50 μl of chemotherapeutic drugs at different concentrations was added to each well Tables 1 and 2, and five wells of each concentration were set as parallel controls (phosphate buffer solution (PBS) instead of chemotherapy drugs), and cultured for 48 h. Sterilized 5 mg/ml MTT in 20 μl was added for a 4-h culture, and DMSO at 150 μl/well

TABLE 2 Drug concentration was determined with MTT sensitivity in Bel-7402/5-Fu cells

Experimental drug	Drug concentration (mg/L)[a]				
5-Fu	250	500	1000	2000	4000
CDDP	2.5	5	10	20	40
MMC	1	2	4	8	16
PTX	2.5	5	10	20	40

[a]The above drug concentration refers to the blood peak concentration and was set after preliminary experiments.

TABLE 3 Drug concentrations applied for apoptosis detection of Bel-7402 cells

Experimental drug	Drug concentration (mg/L)[a]		
5-Fu	25	50	100
CDDP	5	10	20
MMC	1	2	4
PTX	4	8	16

[a]The above drug concentration was determined based on drug sensitivity tests.

TABLE 4 Drug concentrations applied for apoptosis detection of Bel-7402/5-Fu cells

Experimental drug	Drug concentration (mg/L)[a]		
5-Fu	1000	2000	4000
CDDP	10	20	40
MMC	4	8	16
PTX	10	20	40

[a]The above drug concentration was determined based on drug sensitivity tests.

was added to fully dissolve the purple blue crystals. Absorbance (A and A0) at 492 nm was determined using a high-throughput multifunctional microplate test (BMG). A: light absorption value of each drug concentration group, A0: light absorption value of the non-drug group. Experiments were repeated at least three times.

2.4 | Flow cytometry

Bel-7402 and Bel-7402/5-Fu single cell suspensions were centrifuged (112 g) and fixed with 70% ethanol in 3% calf serum at 4°C for 30 min. Cells were centrifuged again (112 g), washed twice with PBS and RNase, and propidium iodide (PI) was added for dark staining for 30 min, and mixed well by vortexing. Finally, cell percentages at G0/G1, S, and G2/M1 phases were detected using flow cytometry (BD).

2.5 | Cell apoptosis assay

Apoptosis was evaluated by staining cells with both Annexin V-FITC and PI according to the manufacturer's instructions. Two-dimensional cells were cultured to logarithmic growth period, and three-dimensional cells were cultured for MCS formation (single cell suspension was prepared for those without intervention). Cells were cultured for 48 h with the following drug concentrations Tables 3 and 4. After digestion of centrifuged cells, 3 ml of PBS was added with 200 µl of binding buffer, 5 µl of Annexin V/FITC, and 10 µl of PI, the mixture was subjected to vortexing, and 300 µl of binding buffer was added. Apoptosis was detected using flow cytometry (BD). PBS was used as negative control. Experiments were repeated at least three times.

2.6 | Analysis of gene expression profiles and signal transduction pathways

Bel-7402 cells and Bel-7402/5-Fu cells were cultured in two and three dimensions. We divided them into sample groups and control groups according to cell type and culture mode. In this experiment, we had two control groups and two sample groups. A1 and A3 were the control groups (A1: two-dimensional cultures with Bel-7402, A3: three-dimensional cultures with Bel-7402); A2 and A4 were the sample groups (A2: two-dimensional cultures with Bel-7402/5-Fu, A4: three-dimensional cultures with Bel-7402/5-Fu). Total RNA from Bel-7402 cells and Bel-7402/5-Fu cells was extracted in strict accordance with the TRIzol (Invitrogen) method.[4] RNA quality was evaluated via electrophoresis on 1.2% agarose formaldehyde gel and quantified via absorbance at A260/A280. Total RNA (5 µg) was reverse transcribed into single stranded DNA using the High-Throughput cDNA preparation kit (Agilent). The preparation and hybridization of fluorescently labeled cRNA were performed using the Cy5 and Cy3 two-color fluorescence labeling methods, respectively. Image scanning was performed using an Axon 4000B scanner. Real-time PCR was performed using Takara Ex Taq R-PCR Version 2.1. GAPDH was used as an endogenous control.

2.7 | Statistical treatment

Spotfire 8.0 and GENMAP software were used to analyze the data. Results are expressed as $\overset{\text{!!}}{x} \pm s$, and SPSS 22.0 statistical software was used to perform a sample *t*-test. $p < .05$ was considered statistically significant.

2.8 | Nomenclature of targets and ligands

Key protein targets and ligands in this article are hyperlinked to corresponding entries in https://www.guidetopharmacology.org/, the common portal for data from the IUPHAR/BPS Guide to PHARMACOLOGY (Harding et al., 2018)[5], and are permanently archived in the Concise Guide to PHARMACOLOGY 2019/20 (Alexander et al., 2019).[6]

3 | RESULTS

3.1 | Morphological characteristics of Bel-7402 and Bel-7402/5-Fu cells under different culture modes

3.1.1 | Morphological characteristics of Bel-7402 cells

In the absence of interfering factors, the two-dimensional cultured cells were larger, grew faster, and showed obvious heteromorphism, most of which were round. TEM showed that the nucleus was larger, the nucleolus ratio was slightly higher (Rnucleus = 3 μm, Rcell = 3.575 μm), and the nucleo-cytoplasmic ratio was about 1.4. The euchromatin in the nucleus was abundant, and the nucleoli could be clearly observed. There were abundant ribosomes in the cytoplasm, small mitochondria, and few rough endoplasmic reticula Figure 1A and B. Under SEM, two-dimensional cultured cells were arranged and dispersed, with wide spacing and occasional intercellular connective structures Figure 1C. Unlike the two-dimensional culture in the absence of interfering factors, the three-dimensional culture showed that cells in suspension clustered and rapidly proliferated, growing into multicellular spheroids (MCSs) of approximately 160–200 μm on the fourth day. TEM showed that the cell morphology was irregular, cell volume was lower than that of cells cultured two-dimensionally, the cell surface was rich in microvilli-like protrusions, and cells were closely connected, with visible capillary bile duct-like structures and desmosome structures Figure 1D and E. Under SEM, cell aggregates were observed to form large irregular masses, small protrusions on the surface of single cells were not obvious, and cells were closely connected Figure 1F.

3.1.2 | Morphological characteristics of Bel-7402/5-Fu cells

In the medium containing 5-Fu 2000 ng/ml, the cell growth rate was slow and the cell heteromorphism was clear in the two-dimensional culture. TEM showed that the cells were round and abundant. There were abundant ribosomes in the cytoplasm, but few mitochondria and rough endoplasmic reticulum. Small spines were observed on the cell surface, and desmogranular desmosome connections were observed between cells Figure 2A and B. Under SEM, two-dimensional cultured cells were arranged and dispersed, and no obvious connecting structure was observed between cells Figure 2C. Compared with cells in the two-dimensional culture, in the medium containing 5-Fu 2000 ng/ml, cells in suspension were clustered in the three-dimensional culture and grew into MCSs of approximately 160–200 μm on the fourth day. TEM showed that the volume of these cells was slightly lower than that of the two-dimensionally cultured cells, the cell shape was irregular, the cell surface was rich in

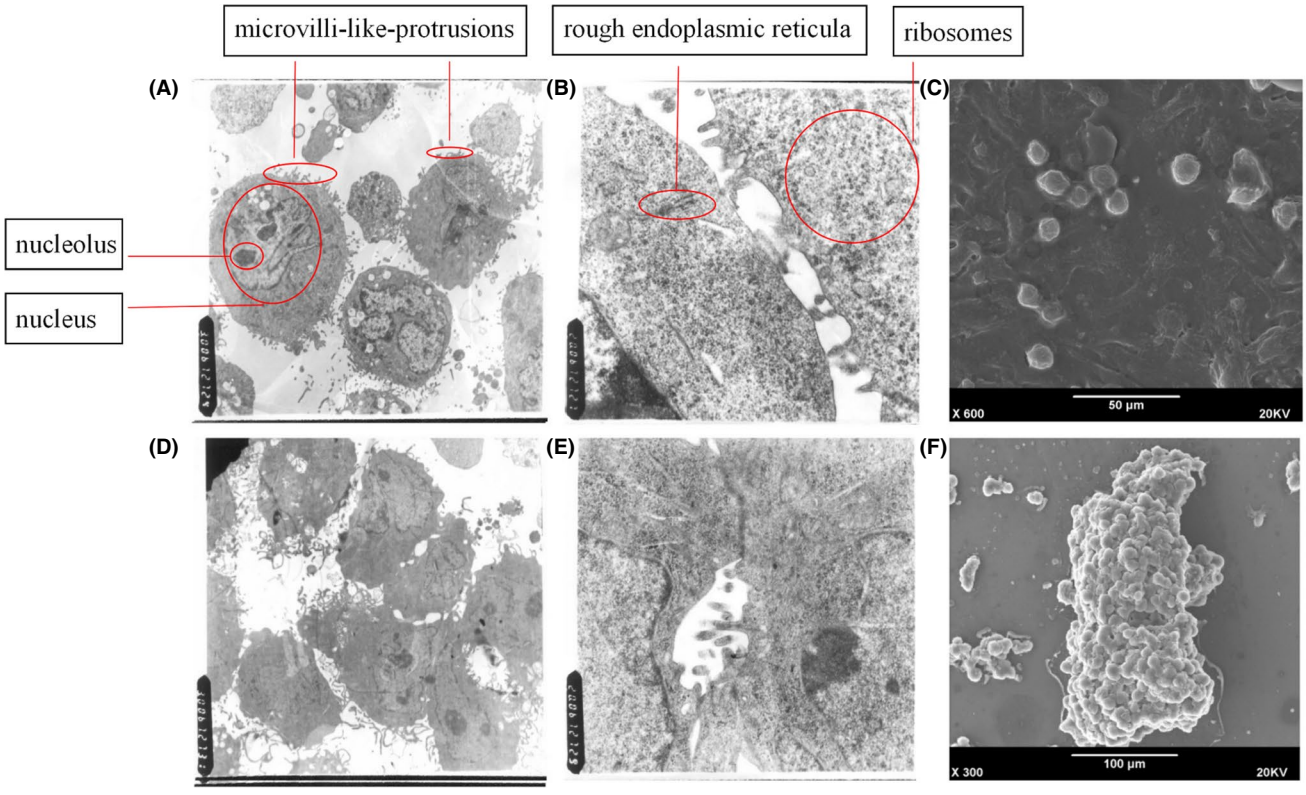

FIGURE 1 Morphological characteristics of Bel-7402 cells under different culture modes. Images of 2d culture with (A) TEM 3000, (B) TEM 20000, and (C) SEM 600 times and of 3d culture with (D) TEM 3000, (E) TEM 20000, and (F) SEM 300

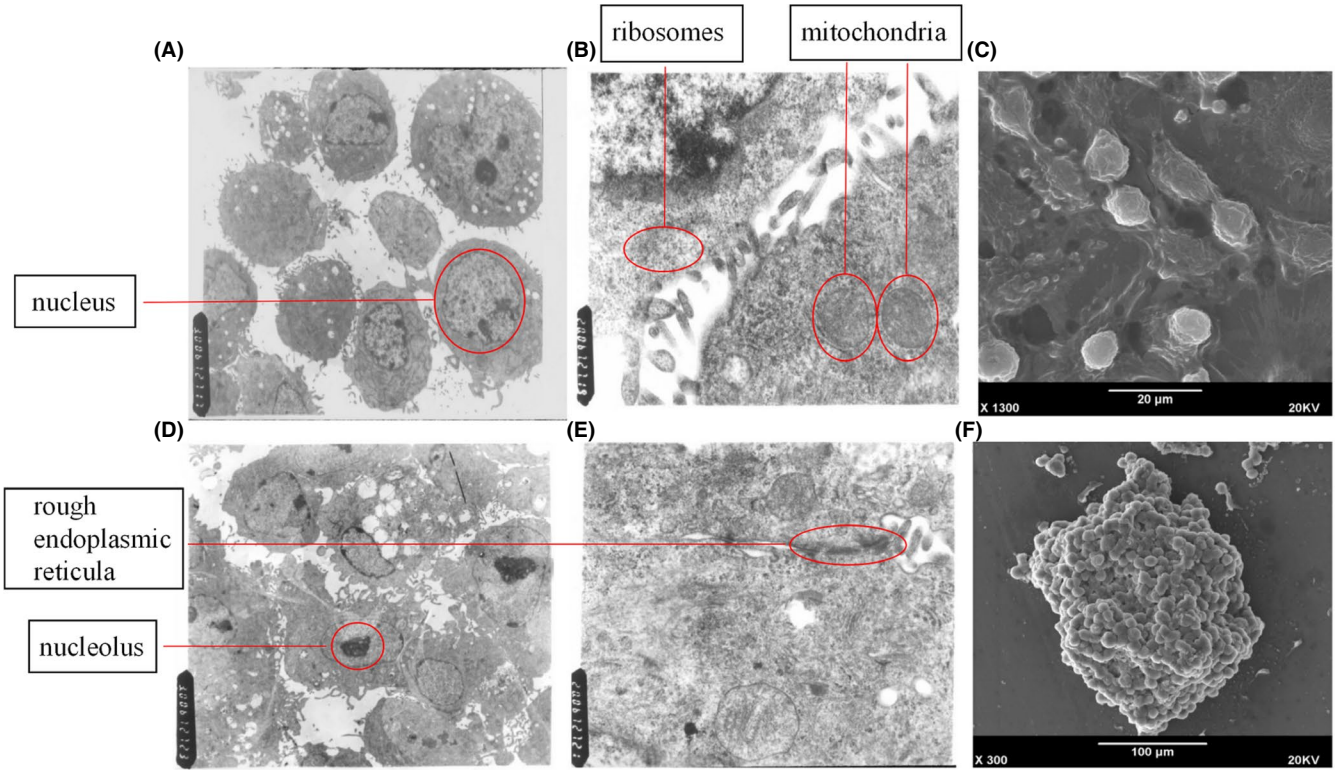

FIGURE 2 Morphological characteristics of Bel-7402/5-Fu cells under different culture modes. Images of 2d cultures with (A) TEM 3000, (B) TEM 20000, and (C) SEM 1300 and of 3d culture with (D) TEM 3000, (E) TEM 20000, and (F) SEM 300

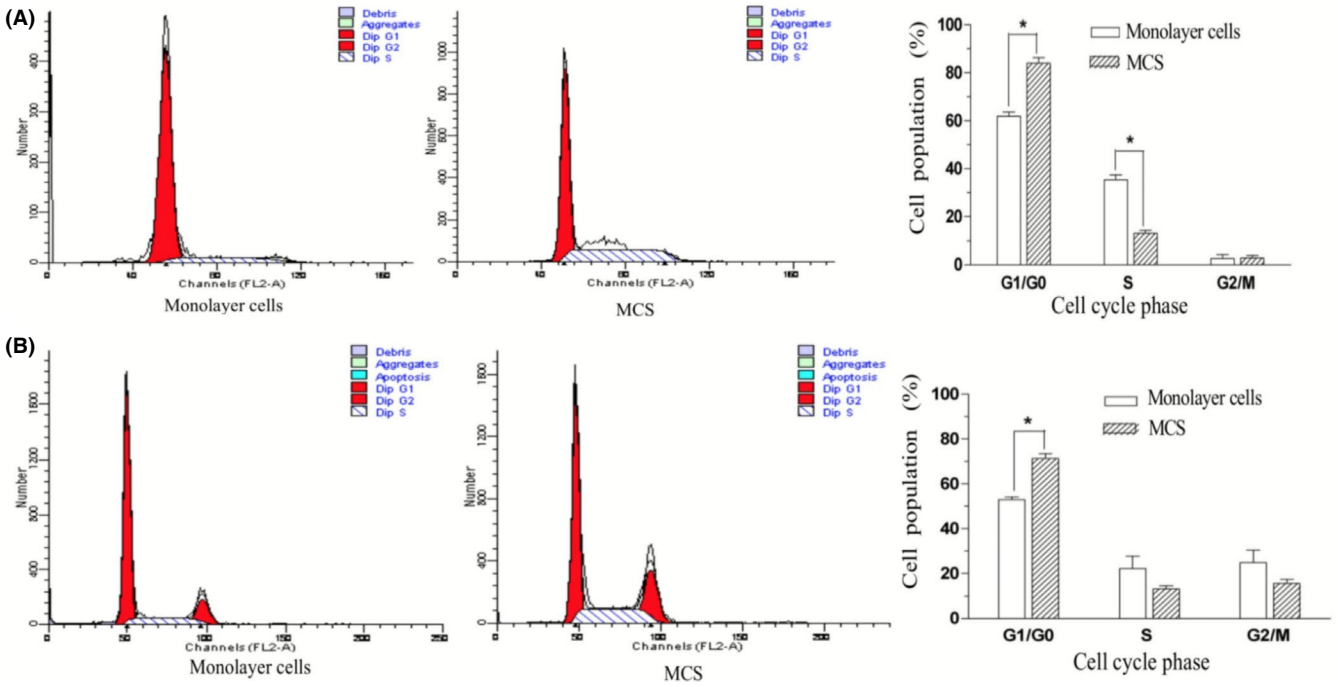

FIGURE 3 Changes in cell cycle distribution of Bel-7402 and Bel-7402/5-Fu cells in the two culture modes. (A) Cell cycle differences of Bel-7402 as determined by flow cytometry in the two culture modes. Graphs represent: Compared with two-dimensional cultured cells, MCS had cell cycle arrest. Cells increased in G1/G0 stage and decreased in S stage ($p < .01$). The cells ratio at G2/M stage changed little ($p > .05$). (B) Cell cycle differences of Bel-7402/5-Fu as determined by flow cytometry in the two culture modes. Graphs represent: Compared with two-dimensional cultured cells, MCS had cell cycle arrest. Cells increased in G1/G0 stage and decreased in S stage ($p < .01$). The cell proportion in S stage and G2/M stage changed little ($p > .05$)

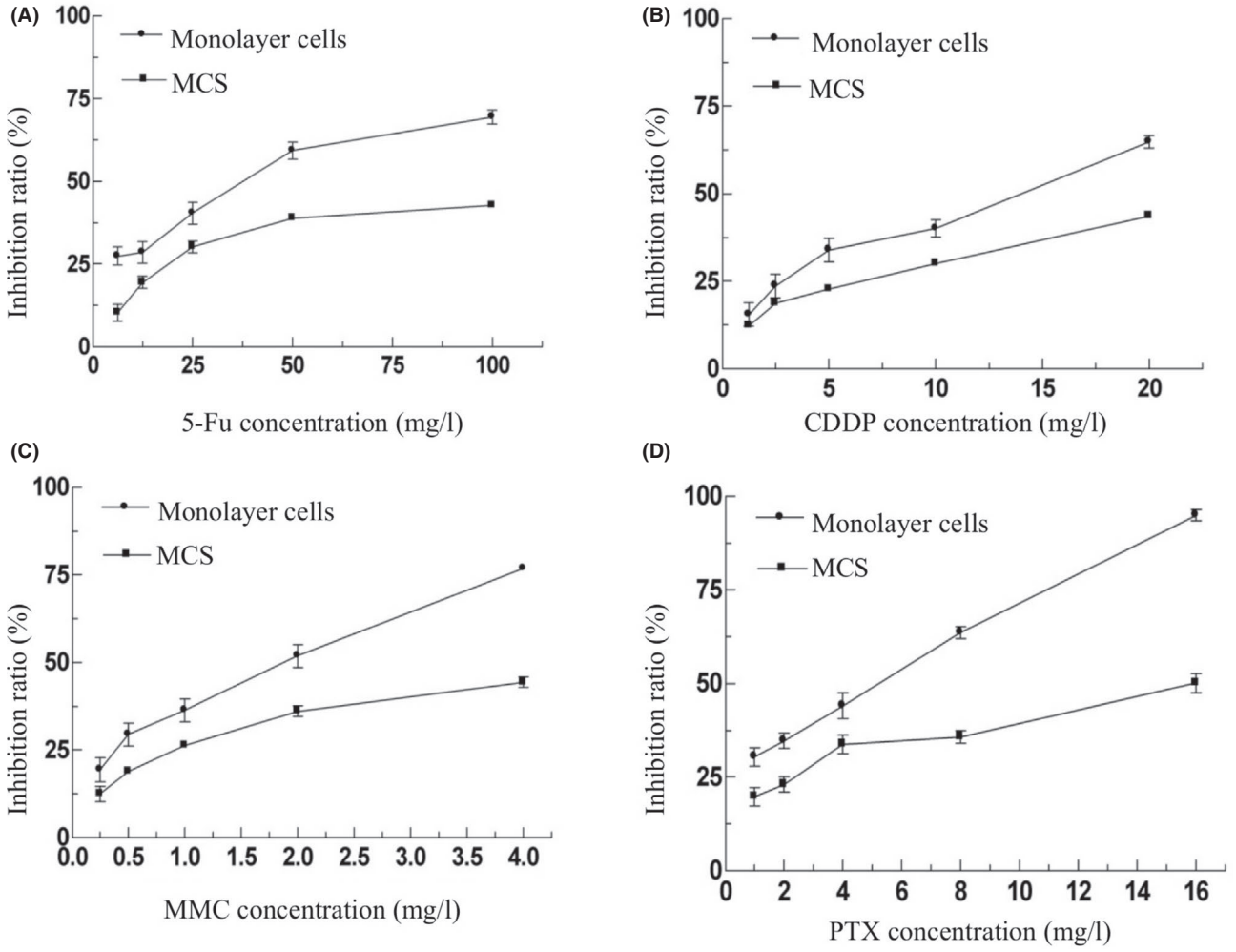

FIGURE 4 Drug sensitivity of Bel-7402 cells was detected by MTT assay under different culture modes. (A) 5-FU, the sensitivity of Bel-7402 cells cultured in 2d to 5-Fu was higher than that in 3d culture groups ($p < .05$). With the increase of drug concentration, the inhibition rate of cells in 2d culture increased gradually, while the upward trend of cell inhibition rate under 3d culture conditions increased slowly; (B) CDDP, the drug sensitivity of Bel-7402 cells cultured in 2d to CDDP was higher than that in 3d cell groups with CDDP concentration >5 mg/L ($p < .05$). At lower CDDP concentrations (1.25 mg/L, 2.5 mg/L), there was no significant difference in the inhibition rate of CDDP on Bel-7402 cells under the two culture modes ($p > .05$); (C) MMC, except for the 0.25 mg/L concentration group, the drug sensitivity of Bel-7402 cells cultured in 2d to MMC was higher than that in 3d culture groups ($p < .05$); and (D) PTX, the sensitivity of Bel-7402 cells cultured in 2d to PTX was higher than that in 3d culture groups ($p < .05$)

microvilli-like protrusions, and the nucleolus was large and obvious Figure 2D and E. Under SEM, we observed multiple spherical cells clustering into large irregular clumps with a rough surface and tight arrangement of cells Figure 2F.

3.2 | Biological characteristics of Bel-7402 and Bel-7402/5-Fu cells under different culture modes

3.2.1 | Cell cycle distribution of Bel-7402 and Bel-7402/5-Fu cells

Compared with two-dimensionally cultured Bel-7402 and Bel-7402/5-Fu cells, MCSs presented cell cycle arrest as follows: G1/G0 phase cells increased ($p < .01$), and G2/M phase cells did not show significant differences ($p > .05$). The S phase changes of Bel-7402 and Bel-7402/5-Fu cells were different. Compared with the two-dimensional culture model, the S phase cells of Bel-7402 cells in the three-dimensional culture decreased ($p < .01$), and the proportion of Bel-7402/5-Fu cells in S phase was mostly unchanged ($p > .05$; Figure 3).

3.2.2 | Drug sensitivity of Bel-7402 and Bel-7402/5-Fu cells

The sensitivity of Bel-7402 and Bel-7402/5-Fu cells to 5-Fu, cisplatin (CDDP), mitomycin (MMC), and paclitaxel (PTX) under different culture modes was assessed using the MTT assay. Two-dimensionally cultured Bel-7402 cells at higher drug concentrations

were significantly more sensitive to the four drugs than those in the three-dimensional culture ($p < .05$). With an increase in the drug concentration, the cell inhibition rate of each group in the two-dimensional culture increased gradually, whereas the same parameter in three-dimensional culture increased slowly, as shown in Figures 4 and 5.

3.2.3 | Apoptotic rate of Bel-7402 and Bel-7402/5-Fu cells

Annexin V/propidine iodide (PI) double staining and flow cytometry revealed no significant difference in spontaneous apoptotic rates of Bel-7402 and Bel-7402/5-Fu cells before drug intervention (PBS was used as negative control) under two- and three-dimensional cultures, as shown in Figure S6. After 48 h of treatment with 5-Fu, CDDP, MMC, and PTX, the apoptosis rate of Bel-7402 cells in the two-dimensional culture was higher than that of cells in the three-dimensional culture. However, no significant difference in apoptosis rate was found between the two-dimensional and three-dimensional cultures at 5 mg/L CDDP, and the apoptosis rate of two-dimensional cultured cells was still higher than that of three-dimensional cultured cells under other drugs. After 48 h of treatment with 5-Fu, CDDP, MMC, and PTX, the apoptosis rate of two and three-dimensionally cultured Bel-7402/5-Fu cells was observed. Apoptosis rates of Bel-7402/5-Fu cells in the two-dimensional cultures were higher than those in the three-dimensional culture cells at various drug concentrations after incubation with 5-Fu, CDDP, and PTX for 48 h. However, there was no significant difference between the apoptosis of the Bel-7402/5-Fu cell group in two-dimensional and three-dimensional culture cell groups at various concentrations of MMC, as shown in Figures S7 and S8.

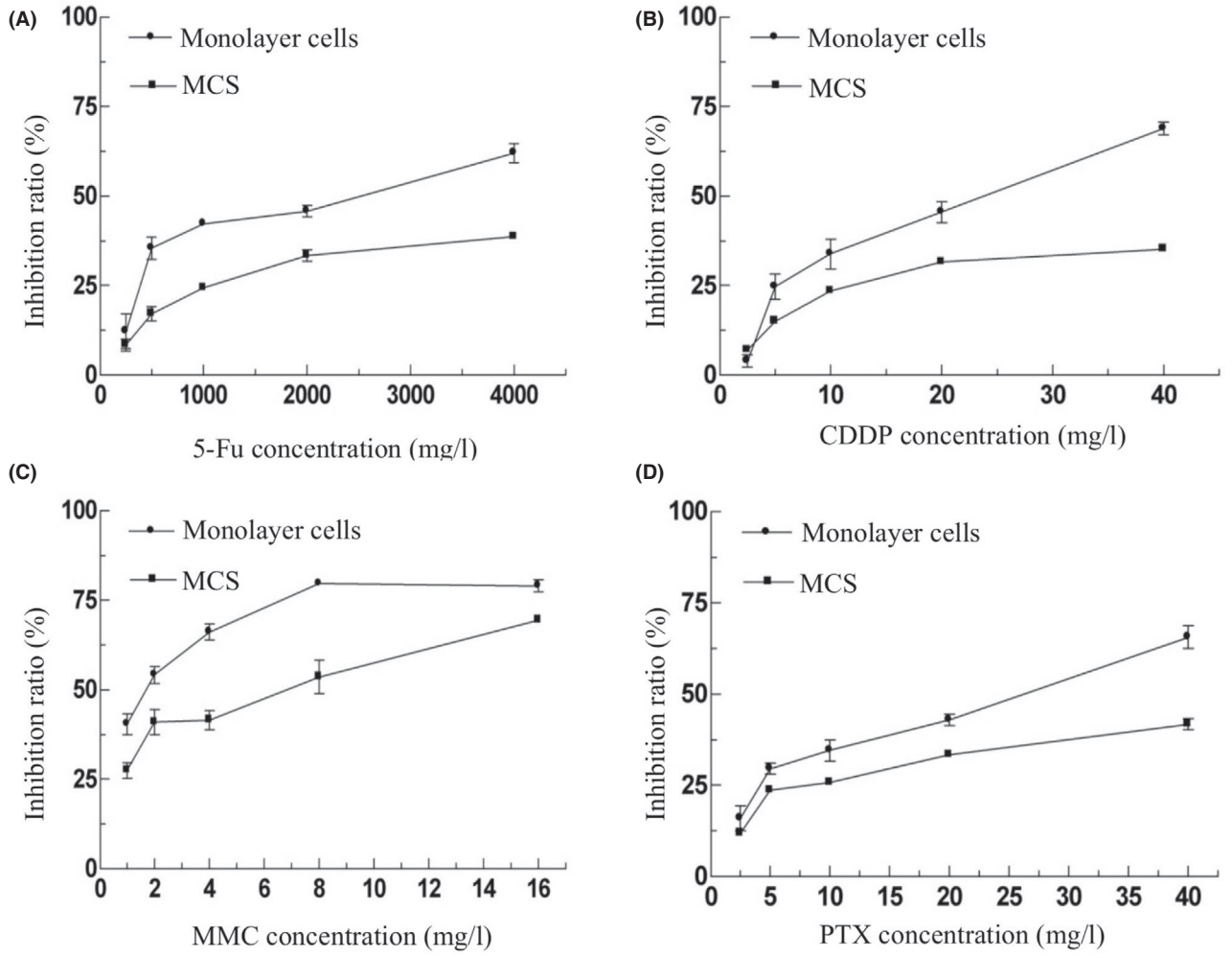

FIGURE 5 Drug sensitivity of Bel-7402/5-Fu cells was detected by MTT assay under different culture modes. (A) 5-FU, except for the 250 mg/L concentration group, the drug sensitivity of Bel-7402/5-Fu cells cultured in 2d to 5-FU was higher than that in 3d culture groups ($p < .05$); (B) CDDP, except for the 2.5 mg/L concentration group, the drug sensitivity of Bel-7402/5-Fu cells cultured in 2d to CDDP was higher than that in 3d culture groups ($p < .05$); (C) MMC, the sensitivity of Bel-7402/5-Fu cells cultured in 2d to MMC was higher than that in 3d culture groups ($p < .05$); and (D) PTX, except for the 2.5 mg/L concentration group, the drug sensitivity of Bel-7402/5-Fu cells cultured in 2d to PTX was higher than that in 3d culture groups ($p < .05$)

3.3 | Gene expression profiles and signal transduction pathways of Bel-7402 and Bel-7402/5-Fu cells under different culture modes

3.3.1 | Gene expression profiles of Bel-7402 and Bel-7402/5-Fu cells

The logarithms of the two groups of data were used as the horizontal and vertical coordinates for the comparison, and the scatter distribution trend was used to intuitively judge the differences between the two groups of data. Genes distributed diagonally along 45° indicate that their expression in both samples was the same. The farther a gene is from the diagonal, the greater is its differential expression in a given copy. Let R = (signal value of sample A2)/(signal value of control A1), the red dot represents $R \geq 2$ (Log$R \geq 0.3$), sample A2 upregulates genes more than two times the expression of control A1. The green dot represents $R \leq 0.5$ (Log$R \leq -0.3$), sample A2 downregulates genes more than 0.5 times the expression of control A1. The blue dot represents $0.5 < R < 2$ ($-0.3 <$ Log$R < 0.3$), sample A2 has no significant differentially expressed genes compared to control A1. (Figure S9). Let R = (signal value of sample A4)/(signal value of control A3), the red dot represents $R \geq 2$ (Log$R \geq 0.3$), sample A4 upregulates genes more than two times the expression of control A3. The green dot represents $R \leq 0.5$ (Log$R \leq -0.3$), sample A4 downregulates genes more than 0.5 times the expression of control A3. The blue dot represents $0.5 < R < 2$ ($-0.3 <$ Log$R < 0.3$), sample A4 has no significant differentially expressed genes compared to control A3. (Figure S10).

In this study, we conducted gene set enrichment analysis by using Genepix Arrat List. The results showed that 47 genes were upregulated and 123 genes were downregulated in the gene expression profile of Bel-7402/5-Fu cells in the two-dimensional culture compared with Bel-7402 cells in the two-dimensional culture. Upregulated genes mainly included histone-related genes, cytoskeleton and motion-related genes, metallothionein genes, metabolic genes, and signal transduction-related genes Table S1. Downregulated genes mainly included metabolic genes, transcription-related genes, cytokine genes, and receptor genes Table S2.

Compared with Bel-7402 cells, Bel-7402/5-Fu MCSs presented 110 upregulated genes and 47 downregulated genes. The former included metabolic genes, transcription-related genes, protein synthesis genes, and modification genes Table S3, whereas the latter included metabolic genes, DNA synthesis and repair genes, and signal transduction-related genes Table S4. The differential genes were analyzed for functional and pathway enrichment using the DAVID bioinformatics database in https://david.ncifcrf.gov/ (Tables S5–S8).

After gene expression profile analysis, four genes (homeobox B2 (HOXB2), proliferating cell nuclear antigen (PCNA), annexin A3 (ANXA3), and trifoliate factor family (TFF1) were selected randomly for quantitative analysis by real-time PCR to verify the results of gene expression profile analysis, using glyceraldehyde-3-phosphate dehydrogenase (GAPDH) as the internal reference. The relative expression rates of the four genes in gene expression profile analysis were all consistent with those of real-time PCR.

3.4 | Signal transduction pathways of Bel-7402 and Bel-7402/5-Fu cells

After Bel-7402 cells developed resistance to 5-Fu, the expression of cyclin D1 (CCND1) was upregulated in the G1 to S cell cycle control signal transduction pathway, cyclin-dependent kinase inhibitor 1C (CDKN1C) and cyclin G2 (CCNG2) genes were downregulated, and there was no significant difference in gene expression in the DNA replication signal transduction pathway. Under MCS culture, the expression of CCND1, minichromosome maintenance protein 2 (MCM2), and minichromosome maintenance protein 3 (MCM3) in the G1 to S cell cycle control signaling pathway was upregulated, and the expression of MCM2 and MCM3 in the DNA replication signaling pathway was upregulated, as shown in Figure S11.

4 | DISCUSSION

4.1 | MCSs are ideal models for studying drug resistance

Liver cancer is one of the most common malignant tumors worldwide. The existence of multidrug-resistant cells is the root cause of the failure of chemotherapy for liver cancer. Therefore, overcoming multidrug resistance of HCC cells has become an urgent task. It is necessary not only to elucidate the drug resistance mechanism of individual cancer cells but also to consider the interaction and cooperation between cells.

In this study, a three-dimensional culture method was used to maintain Bel-7402 and Bel-7402/5-Fu HCC cells. We observed that the cultured cells in suspension aggregated and rapidly proliferated. The morphology of these cells was irregular, and they were tightly connected and smaller than two-dimensionally cultured cells. Studies have shown that owing to the specific structure and characteristics of many cancer cell lines in the three-dimensional culture, their sensitivity to chemotherapeutic drugs is substantially lower than that of the same cell lines in the two-dimensional culture.[7,8] This mechanism of drug resistance, called MCR exists in the population structure in which tumor cells are related to each other.

The MTT method was used to evaluate the sensitivity of cells to 5-Fu, CDDP, MMC, and PTX in different culture modes. We found that the sensitivity of Bel-7402 cells in the two-dimensional culture at higher drug concentrations to the four drugs was significantly higher than that of cells in the three-dimensional culture. With the increase of drug concentration, the cell inhibition rate of each group gradually increased, and the cell inhibition rate increased slowly under three-dimensional culture conditions; at lower drug concentrations, no significant difference in the cell inhibition rate between the two culture methods was found. The main reason for this result

was that the drug concentration did not reach an effective inhibitory concentration. Moreover, Bel-7402/5-Fu cells developed resistance not only to 5-Fu but also to other cancer drugs with different chemical structures and action mechanisms, such as CDDP, to which they had never been exposed to, indicating that these cells present multidrug resistance (MDR) characteristics and can maintain drug resistance. This suggests that the assessment of drug sensitivity in three-dimensional cultures might better reflect the characteristics of tumors in vivo, providing a more reliable basis for the discovery of new targets in solid tumors in vivo.[9,10]

The findings of Lee et al[11] and Meli et al[12] on the three-dimensional culture of human HepG2 hepatoma cells show that three-dimensionally cultured cells are easy to aggregate into multicellular spheres, which is consistent with our findings on cell morphology observed in three-dimensional cultures. A study of head and neck squamous cell carcinoma (HNSCC) tumors in two- and three-dimensional culture systems showed that cells cultured in these two culture modes have significant differences in survival, apoptosis, and drug response and some genetic changes. They found that HNSCC cells in the three-dimensional culture were spheroids, and most cell lines were significantly less sensitive to cisplatin and cetuximab than those in the two-dimensional culture. This may be closely related to the increase of cancer stem-like cell (CSC)-related proteins and downregulation of epidermal growth factor receptor (EGFR) in the three-dimensional culture.[13] A number of studies have shown that the three-dimensional cell culture model can better mimic the tissue environment, improve cell function (in vitro) and intuitively intervene and manipulate the cells, which is beneficial to the growth, proliferation, and differentiation of liver cancer cells, thereby enabling the study of MCR mechanism in liver cancer.[14–16] In summary, the MCR model of liver cancer established in this study is successful, representing an ideal MCR cell-based model for studying drug resistance mechanisms and screening reversal agents.

4.2 | MCS mechanism leading to tumor cell resistance

In this study, the cell cycle distribution of Bel-7402 and Bel-7402/5-Fu cells in two different culture models was measured by flow cytometry. We found a cell cycle blockage in cells in the three-dimensional culture compared with those in the two-dimensional culture, especially in the G1/G0 phase. The proportion of cells in G2/M phases did not change significantly. Consistent with the results of Lee et al,[17] a study on 5-FU resistance in a 3D colorectal adenocarcinoma model, the changes in cell cycle distribution of the DLD-1 (human colon adenocarcinoma cells) were evident, showing G1 cell cycle arrest with a significant decrease in the percentage of S and G2/M phase cells.

The results also indicated that there was no significant difference in the spontaneous apoptosis rate of Bel-7402 and Bel-7402/5-Fu cells before drug intervention between the two culture modes, which may result from the lack of stimulation that effectively induces apoptotic agents. Tumor cells can tolerate chemotherapeutic drugs by inhibiting apoptosis, one of the self-protection mechanisms of tumor cells. However, when chemotherapeutic drugs act on Bel-7402 and Bel-7402/5-Fu cells, the apoptosis rate of two-dimensionally cultured cells is, in general, higher than that of three-dimensionally cultured cells, which also strongly confirms that the MCS culture can inhibit chemotherapy-induced tumor cell apoptosis, which is one of the mechanisms of MCR. In this case, the specific underlying drug resistance mechanism may be the increase of cell-to-cell and/or cell-to-matrix contact in the three-dimensional culture, leading to hypoxia. This hypothesis is consistent with the research by Watson et al,[18] who found that when glioblastoma cells are cultured in three dimensions, they present evident resistance to temozolomide, which is caused by hypoxia. Similar to the above results, Chiew et al obtained a HCC tumor microenvironment with a hypoxic core and a true drug-penetration gradient in a three-dimensional culture system of liver cancer cells that can be used for drug screening.[19]

4.3 | Mechanism of multicellular drug resistance in liver cancer

In this study, the analysis of signal transduction pathways showed that anti-tumor drugs can upregulate CCND1, MCM2, and MCM3 and downregulate CDKN1C and CCNG2 in the G1 to S cell cycle control signal transduction pathway in Bel-7402/5-Fu cells. In addition, MCM2 and MCM3 were upregulated in the DNA replication signal transduction pathway. Therefore, the mechanism of MCR acquired by our liver cancer Bel-7402/5-Fu cell model may be closely related to the activation of these two signal transduction pathways.

The formation of tumors is mainly triggered by dysregulation of signal transduction pathways in the G1 to S phases of the cell cycle, and the CCND1 gene-encoded protein (cyclin D1) is the first cyclin synthesized by the cell in the proliferation cycle, exerting a significant effect on cell proliferation and apoptosis. Cyclin D1 is synthesized in the G1 phase and then forms a protein complex with cyclin-dependent kinase (CDK)4/6, which regulates the G1/S phase of the cell cycle. When the cell enters the S phase, cyclin D1 is degraded in the cytoplasm, and thus CCND1 plays a vital role in regulating the G1/S phase.[20] Autophagy, a conserved process in cell evolution, maintains intracellular homeostasis by degrading defective organelles and other harmful aggregates but also reduces the stress of cancer cells to promote tumor development. Studies on the HCC oncogene CCND1 (encoding cyclin D1) and autophagy in the regulation of the differentiation of liver cancer stem cells (LCSCs) indicated that the expression of CCND1 in liver cancer cell lines is higher than that in normal liver cells and that CCND1 gene silencing is inhibited by autophagy. The differentiation of LCSCs inhibits the proliferation of liver cancer cells in vitro and tumor growth and delays the development of HCC.[21] Wu's team[22] used 147 tumor tissue samples from HCC patients and three mouse models to reveal a negative correlation between

low autophagy activity and high CCND1 expression. Their analysis showed that tumor cells activate autophagy by degrading ubiquitinated CCND1, which plays an inhibitory role in cell proliferation, colony formation, and tumorigenesis. As an oncogene in liver cancer cells, CCND1 participates in different signaling pathways and plays a corresponding role in the G1 phase of the cell cycle. For example, some studies have shown that overexpression of mitogen-inducible gene 6 (MIG-6) can lead to significant G1 arrest and growth inhibition in HCC cells by inhibiting the phosphorylated ERK (p-ERK) and cyclin D1 pathways, whereas eukaryotic translation elongation factor 1A1 (eEF1A1) regulates the G1 phase of the cell cycle through the signal transducer and activator of transcription 1 (STAT1)-cyclin D1 signaling pathway, thus promoting tumor proliferation.[23,24] It is clear that CCND1 has become a potential target for tumor therapy.

CDKN1C encodes the $p57^{KIP2}$ protein, a CDK inhibitor that negatively regulates the cell cycle and regulates cell proliferation, transcription, apoptosis, differentiation, development, and cell migration in a variety of human cancers, including HCC.[25] Giovannini et al[26] showed that CDKN1C/p57 can regulate the activity of HCC cells through two target genes, Notch 1 Signaling pathway (NOTCH1) and Notch 3 Signaling pathway (NOTCH3). Their results show that the upregulation of the CDKN1C/p57 gene can lead to reduced cell line growth and apoptosis. In contrast, CDKN1C/p57 gene downregulation promotes the proliferation of liver cancer cells. In an experiment evaluating the expression of Jun activation domain-binding protein 1 (JAB1) and p57 in a series of HCC tissues, the expression of JAB1 was found to be negatively correlated with that of CDKN1C/p57. In HCC, abnormal expression of JAB1 can significantly reduce CDKN1C/p57 levels and promote tumor cell growth.[27] The decrease and absence of CDKN1C protein expression in HCC tissues indicate that the relationship between CDKN1C and liver cancer needs further investigation and that CDKN1C can be used as one of the independent prognostic factors in HCC patients.

Cyclin G2 (CCNG2) is a relatively late member of the cyclin family. In recent years, it has been found that CCNG2 can inhibit cell proliferation and promote apoptosis, and its expression can inhibit the transformation of the G1/S phase and negatively regulate the proliferation of tumor cells. The deletion of CCNG2 may lead to the occurrence of some malignancies. Gao et al discovered that CCNG2 inhibits the growth and migration of gastric cancer cells by inhibiting Wnt/β-catenin signaling. In gastric cancer tissues, the expression level of CCNG2 is related to poor tumor size, migration, and differentiation status.[28] Nevertheless, there are few reports on CCNG2 and liver cancer. It is therefore necessary to further study their relationship and clarify the possible involvement in liver cancer drug resistance, so as to grasp the role of CCNG2 in exerting anti-tumor effects.

It is well established that the MCM protein family is one of the essential factors for the initiation and extension of DNA replication. The expression of MCM proteins is an important target of the cell's proliferation ability.[29] A large number of studies have shown that MCM genes play an important role in various cancers, especially in cancer diagnosis and prognosis prediction,in liver cancer tissues, all MCM genes are significantly upregulated, indicating their potential diagnostic value.[30,31] In a study exploring differentially expressed genes in liver cancer, the authors found that MCM3 and MCM2 expression is negative in normal tissues and positive in HCC tissues and that overexpression of MCM2 and MCM3 in liver cancer tissues can be related to low survival rates and tumor progression in these patients.[32] Zhuang et al used the gene expression omnibus (GEO) and the cancer genome atlas (TCGA) databases to analyze 13 genes related to liver cancer and concluded that the upregulation of MCM3 in HCC tissues is closely related to poor histological grade of liver cancer and the deterioration of overall survival (OS) and disease-free survival (DFS) of HCC patients.[33] It is speculated that MCM3 should be the new prognostic biomarker and target for the treatment of HCC patients. Moreover, Yang's team used quantitative proteomics to identify differentially expressed proteins in HCC tumor tissues and found that among the upregulated tumor-associated proteins, MCM2 was one of the most significantly altered proteins, with its overexpression being detected by tissue microarray.[34] Through MCM2 immunostaining, the expression of this protein was confirmed in 12 pairs of HCC patients' tumors and adjacent tissues. Immunostaining showed that the expression of MCM2 in advanced HCC tumors was significantly higher than that in early-stage tumors. Additionally, MCM2 can reduce the proliferation of liver cancer cells through the CDK pathway and block the cell cycle in the S phase. In accordance with the function of the MCM gene, the expression of MCM2 and MCM3 in the G1 to S cell cycle control signal transduction pathway and DNA replication signal transduction pathway is upregulated in our experiments, indicating that overexpression of MCM2 and MCM3 will cause DNA replication errors, further leading to uncontrolled cell proliferation. This suggests that the overexpression of MCM2 and MCM3 may be one of the mechanisms underlying MCR in Bel-7402 cells.

In a study on the ability of (+)-terrein to inhibit liver cancer cell proliferation by blocking the cell cycle, gene expression analysis and evaluation of cell cycle-related genes and cell morphology-related genes, including CCND1, MCM2, MCM3, and CDKN1C, were performed. The study showed that the effect of (+)-terrein on cell cycle was reflected by the decreased proportion of cells in the G0/G1 phase and S phase, whereas the proportion of cells in the G2/M phase increased. The author used the pathview package to create the cell cycle path map, which confirmed that CDKN1C was downregulated in the cell cycle and CCND1, MCM2, and MCM3 could be upregulated genes.[35] Therefore, the results presented in the abovementioned study are in accordance with our findings,the correlation may be positive or negative with respect to the related signaling pathway of phosphorylation and dephosphorylation, methylation and demethylation, and ubiquitination role, which needs to be further explored and verified.

The molecular mechanisms of upregulation and downregulation of the above genes may involve JAK/STAT, PI3 K/Akt and MAPK signaling pathway, suggesting that the growth and apoptosis of liver cancer can be realized through multi-target and multi-signaling

pathways. At present, some related studies have reported the mutual activation and regulation of these genes and the main signaling pathways in tumors. For example, Yang[36] confirmed that CCND1 can activate the activity of MAPK/PI3 K-Akt signaling pathway in tumor progression in Lung squamous cell cancer. However, there are few studies on liver cancer, so we need to make further and deeper exploration. We used Kegg Pathway Database (https://www.genome.jp/kegg/pathway.html) and our experimental results to draw the diagram of signal transduction pathway.

Many "signals" on the surface of HCC cells and drug-resistant cells act as suppressors of immune cells, preventing the destruction of tumors. In addition to programmed cell death-1 (PD-1), programmed death ligand 1 (PD-L1) and cytotoxic T-lymphocyte-associated protein 4 (CTLA-4), the genes encoding proteins that participate in signal transduction pathways may also serve as new immune checkpoints and can be used as new and independent prognostic factors for liver cancer. Whether regulating the activity of key genes in signal transduction pathways can effectively reverse MCR in HCC remains unclear. Finding these potential targets and signaling pathways is one of the important future directions of tumor immunotherapy research.

5 | CONCLUSIONS

Through different cell culture models and proliferation and apoptosis experiments, MCS culture was found to be an ideal model for studying multicellular drug resistance in liver cancer. However, there are some shortcomings in this study. The exact effect of intercellular connectivity structure in MCR is not clear, and needs further scrutiny. Only one time point in MCS growth was selected to measure its cell cycle, and the changes in cell proportion at each stage with culture time were not observed. Chemotherapy drugs can induce the death of tumor cells by inducing apoptosis, whereas MCS can inhibit or delay apoptosis. Therefore, further experiments are needed to clarify whether MCS can be used as a means of individualized treatment for anti-tumor drugs. Studies show that organoid culture, rather than three-dimensional culture, is the culture method that most closely resembles the human tumor environment, as it allows differentiation and spontaneous formation of structures that are highly similar to the source tissues or organs in the body, and is very effective in drug screening for the patients' treatments. However, because of the technical difficulty and high cost of this method, it has not been widely used in research. Moreover, the gene expression profile of Bel-7402 and Bel-7402/5-Fu cells in different culture conditions enabled us to infer about the possible mechanism of MCR. However, this study did not evaluate the biological characteristics of differentially expressed genes in liver cancer to determine the specific functions of these genes. In addition, the differentially expressed genes of the signal transduction pathway were not perturbed to observe their effect on drug resistance in HCC cells. Therefore, we need to further study the above issues, regulate the activity of genes in key parts of the signal transduction pathway, and observe whether it can effectively reverse the MCR of liver cancer, so as to find new molecular markers and therapeutic targets suitable for early diagnosis to improve prognosis and quality of life.

CONFLICT OF INTEREST

The author(s) declared no potential conflicts of interest with respect to the research, authorship, and/or publication of this article.

AUTHOR CONTRIBUTIONS

Chunli Li, Nan Mei and Ni Zhao conceived the study. Nan Mei and Tao Tian performed the experiments. Ni Zhao and Min Jiao collected and analyzed the data. Chunli Li provided the funding and supervised the study. Nan Mei wrote the original draft. Ni Zhao, Tao Tian and Min Jiao reviewed and edited the manuscript. All authors read and approved the final manuscript.

DATA AVAILABILITY STATEMENT

The datasets and data used and analyzed in this study are available from the corresponding author on reasonable request.

ORCID

Chunli Li https://orcid.org/0000-0001-8488-1674

REFERENCES

1. Ryerson AB, Eheman CR, Altekruse SF, et al. Annual Report to the Nation on the Status of Cancer, 1975–2012, featuring the increasing incidence of liver cancer. *Cancer*. 2016;122:1312-1337.
2. Ravi M, Ramesh A, Pattabhi A. Contributions of 3D cell cultures for cancer research. *J Cell Physiol*. 2017;232:2679-2697.
3. Nath S, Devi GR. Three-dimensional culture systems in cancer research: focus on tumor spheroid model. *Pharmacol Ther*. 2016;163:94-108.
4. Walker J, Martin C, Callaghan R. Inhibition of P-glycoprotein function by XR9576 in a solid tumour model can restore anticancer drug efficacy. *Eur J Cancer*. 2004;40:594-605.
5. Harding SD, Sharman JL, Faccenda E, et al. The IUPHAR/BPS Guide to PHARMACOLOGY in 2018: updates and expansion to encompass the new guide to IMMUNOPHARMACOLOGY. *Nucleic Acids Res*. 2018;46:D1091-D1106.
6. Alexander SPH, Mathie A, Peters JA, et al. THE CONCISE GUIDE TO PHARMACOLOGY 2019/20: ion channels. *Br J Pharmacol*. 2019;176(S1):S142-S228.
7. Kundu B, Saha P, Datta K, Kundu SC. A silk fibroin based hepatocarcinoma model and the assessment of the drug response in hyaluronan-binding protein 1 overexpressed HepG2 cells. *Biomaterials*. 2013;34:9462-9474.
8. Barrera-Rodriguez R, Fuentes JM. Multidrug resistance characterization in multicellular tumour spheroids from two human lung cancer cell lines. *Cancer Cell Int*. 2015;15:47.
9. Yip D, Cho CH. A multicellular 3D heterospheroid model of liver tumor and stromal cells in collagen gel for anti-cancer drug testing. *Biochem Biophys Res Commun*. 2013;433:327-332.
10. Sant S, Johnston PA. The production of 3D tumor spheroids for cancer drug discovery. *Drug Discov Today Technol*. 2017;23:27-36.
11. Lee D, Pathak S, Jeong JH. Design and manufacture of 3D cell culture plate for mass production of cell-spheroids. *Sci Rep*. 2019;9:13976.
12. Meli L, Jordan ET, Clark DS, Linhardt RJ, Dordick JS. Influence of a three-dimensional, microarray environment on human cell culture in drug screening systems. *Biomaterials*. 2012;33:9087-9096.
13. Melissaridou S, Wiechec E, Magan M, et al. The effect of 2D and 3D cell cultures on treatment response, EMT profile and stem cell features in head and neck cancer. *Cancer Cell Int*. 2019;19:16.

14. Gunness P, Mueller D, Shevchenko V, Heinzle E, Ingelman-Sundberg M, Noor F. 3D organotypic cultures of human HepaRG cells: a tool for in vitro toxicity studies. *Toxicol Sci*. 2013;133:67-78.
15. Mueller D, Krämer L, Hoffmann E, Klein S, Noor F. 3D organotypic HepaRG cultures as in vitro model for acute and repeated dose toxicity studies. *Toxicol in Vitro*. 2014;28:104-112.
16. Fang M, Peng CW, Liu SP, Yuan JP, Li Y. In vitro invasive pattern of hepatocellular carcinoma cell line HCCLM9 based on three-dimensional cell culture and quantum dots molecular imaging. *J Huazhong Univ Sci Technol Med Sci*. 2013;33:520-524.
17. Lee SH, Nam JK, Park JK, Lee JH, Min DS, Kuh H-J. Differential protein expression and novel biomarkers related to 5-FU resistance in a 3D colorectal adenocarcinoma model. *Oncol Rep*. 2014;32:1427-1434.
18. Musah-Eroje A, Watson S. A novel 3D in vitro model of glioblastoma reveals resistance to temozolomide which was potentiated by hypoxia. *J Neurooncol*. 2019;142:231-240.
19. Chiew GGY, Wei N, Sultania S, Lim S, Luo KQ. Bioengineered three-dimensional co-culture of cancer cells and endothelial cells: a model system for dual analysis of tumor growth and angiogenesis. *Biotechnol Bioeng*. 2017;114:1865-1877.
20. Musgrove EA, Caldon CE, Barraclough J, Stone A, Sutherland RL. Cyclin D as a therapeutic target in cancer. *Nat Rev Cancer*. 2011;11:558-572.
21. Zhang H. CCND1 silencing suppresses liver cancer stem cell differentiation through inhibiting autophagy. *Human Cell*. 2020;33:140-147.
22. Wu SY, Lan SH, Wu SR, et al. Hepatocellular carcinoma-related cyclin D1 is selectively regulated by autophagy degradation system. *Hepatology*. 2018;68:141-154.
23. Huang J, Zheng C, Shao J, Chen L, Liu X, Shao J. Overexpression of eEF1A1 regulates G1-phase progression to promote HCC proliferation through the STAT1-cyclin D1 pathway. *Biochem Biophys Res Commun*. 2017;494:542-549.
24. Li Z, Qu L, Luo W, et al. Mig-6 is down-regulated in HCC and inhibits the proliferation of HCC cells via the P-ERK/Cyclin D1 pathway. *Exp Mol Pathol*. 2017;102:492-499.
25. Stampone E, Caldarelli I, Zullo A, et al. Genetic and epigenetic control of CDKN1C expression: Importance in cell commitment and differentiation, tissue homeostasis and human diseases. *Int J Mol Sci*. 2018;19:1055.
26. Giovannini C, Gramantieri L, Minguzzi M, et al. CDKN1C/P57 is regulated by the Notch target gene Hes1 and induces senescence in human hepatocellular carcinoma. *Am J Pathol*. 2012;181:413-422.
27. Guo H, Jing L, Cheng Y, et al. Down-regulation of the cyclin-dependent kinase inhibitor p57 is mediated by Jab1/Csn5 in hepatocarcinogenesis. *Hepatology*. 2016;63:898-913.
28. Gao J, Zhao C, Liu Q, et al. Cyclin G2 suppresses Wnt/β-catenin signaling and inhibits gastric cancer cell growth and migration through Dapper1. *J Exp Clin Cancer Res*. 2018;37:317.
29. Ishimi Y. Regulation of MCM2-7 function. *Genes Genet Syst*. 2018;93:125-133.
30. Belinky F, Nativ N, Stelzer G, et al. PathCards: multi-source consolidation of human biological pathways. *Database (Oxford)*. 2015;2015:bav006.
31. Liao X, Liu X, Yang C, et al. Distinct diagnostic and prognostic values of minichromosome maintenance gene expression in patients with hepatocellular carcinoma. *J Cancer*. 2018;9:2357-2373.
32. Yang WX, Pan YY, You CG. CDK1, CCNB1, CDC20, BUB1, MAD2L1, MCM3, BUB1B, MCM2, and RFC4 may be potential therapeutic targets for hepatocellular carcinoma using integrated bioinformatic analysis. *Biomed Res Int*. 2019;2019:1245072.
33. Zhuang L, Yang Z, Meng Z. Upregulation of BUB1B, CCNB1, CDC7, CDC20, and MCM3 in tumor tissues predicted worse overall survival and disease-free survival in hepatocellular carcinoma patients. *Biomed Res Int*. 2018;2018:7897346.
34. Yang J, Xie Q, Zhou H, et al. Proteomic analysis and NIR-II imaging of MCM2 protein in hepatocellular carcinoma. *J Proteome Res*. 2018;17:2428-2439.
35. Zhang F, Mijiti M, Ding W, et al. (+)-Terrein inhibits human hepatoma Bel-7402 proliferation through cell cycle arrest. *Oncol Rep*. 2015;33:1191-1200.
36. Yang Y, Lu T, Li Z, et al. FGFR1 regulates proliferation and metastasis by targeting CCND1 in FGFR1 amplified lung cancer. *Cell Adh Migr*. 2020;14(1):82-95.

SUPPORTING INFORMATION

Additional supporting information may be found online in the Supporting Information section.

How to cite this article: Mei N, Zhao N, Tian T, Jiao M, Li C. Biological features, gene expression profile, and mechanisms of drug resistance of two- and three-dimensional hepatocellular carcinoma cell cultures. *Pharmacol Res Perspect*. 2021;9:e00715. https://doi.org/10.1002/prp2.715